Retinal scanning laser polarimetry and methods to compensate for corneal birefringence

ZHOU Q.[1,2]

ABSTRACT

Scanning laser polarimetry (SLP) was developed to provide objective assessment of the retinal nerve fiber layer (RNFL), a birefringent tissue, by measuring the total retardation in the reflected light. The birefringence of the anterior segment of the eye, mainly the cornea, is a confounding variable to the RNFL measurement. Anterior segment birefringence varies over a wide range among individuals. This paper reviews the principle of SLP and methods to measure and compensate for anterior segment birefringence as implemented in a commercial SLP system, GDx VCC. Anterior segment birefringence is measured from the macular retardance profile. It can be neutralized with a variable retarder in the GDx VCC and the measured retardance directly represents the RNFL retardance. Alternatively, a bias retarder can be introduced in the measurement beam path with approximately vertical slow axis, SLP measures the combination of the RNFL and the bias retarder, and RNFL retardance is then mathematically extracted from the measurement. The latter has the advantage of improved signal-to-noise ratio. With the combination of a visual RNFL image and rapid, objective, and reproducible assessment of the RNFL, GDx VCC provides an attractive clinical tool in glaucoma management.

KEYWORDS

Scanning laser polarimetry, retinal birefringence, light retardation, retinal nerve fiber layer, glaucoma, anterior segment birefringence

RÉSUMÉ

La polarimétrie à balayage laser (PBL) a été développée pour permettre d'estimer la couche de fibres nerveuses rétiniennes (CFNR), un tissu biréfringent, en mesurant le retard total dans la lumière réfléchie. La biréfringence du segment antérieur de l'œil, principalement la cornée, représente une variable confusionnelle pour la mesure de la CFNR. La biréfringence du segment antérieur varie sur une large gamme selon les individus. Cet article examine le principe de la PLB et les procédés permettant de mesurer et de compenser la biréfringence du segment antérieur tel qu'il est réalisé dans un système commercial de PLB, le GDx VCC. La biréfringence du segment antérieur est mesurée à partir du profil de retard maculaire. Elle peut être neutralisée avec un retardateur variable dans le GDx VCC et le retard mesuré représente directement le retard de la CFNR. En variante, un retardateur de polarisation peut être introduit dans la trajectoire des faisceaux de mesure selon un axe lent pratiquement vertical, la PBL mesure la combinaison de la CFNR et du retardateur de polarisation, et le retard de la CFNR est alors obtenu mathématiquement à partir de la mesure. Ce dernier a l'avantage de générer un meilleur rapport signal/bruit. Utilisé en combinaison avec une image visuelle de la CFNR et une estimation rapide, objective et reproductible de la CFNR, le GDx VCC est un outil clinique attrayant pour le traitement du glaucome.

.....

[1] *Laser Diagnostic Technologies Inc., San Diego, CA*
[2] *R&D,Carl Zeiss Meditec Inc, ,San Diego, CA*

MOTS-CLÉS

Polarimétrie à balayage laser, biréfringence rétinienne, retard de lumière, couche de fibres nerveuses rétiniennes, glaucome, biréfringence du segment antérieur

INTRODUCTION

Glaucoma is a multifactorial optic neuropathy characterized by progressive loss of the retinal ganglion cells (RGCs) and thinning of the retinal nerve fiber layer (RNFL), leading to visual field loss and eventually, total loss of vision. Damage to the retinal tissue by glaucoma is irreversible. It is crucial to detect the disease early to initiate appropriate treatment and to closely monitor progression to assess treatment efficacy. It has long been recognized that abnormalities in the retinal nerve fiber layer reveal the earliest sign of glaucoma damage.[16] Nearly half of the optic nerve fibers in the eye may be lost before recognizable optic nerve head (ONH) abnormalities and detectable visual field loss.[24-26,30]

The RNFL consists of bundles of ganglion cell axons. In a red-free fundus photograph, the nerve fiber bundles appear as bright striations converging towards the optic nerve head (ONH) (Fig. 1), where brighter striations correspond to thicker RNFL bundles. In a normal eye, the nerve fiber layer is thicker in the superior and inferior peripapillary regions and thinner in the temporal and nasal peripapillary regions.

The nerve fiber bundles contain microtubules, cylindrical intracellular organelles with diameter much smaller than the wavelength of the illuminating light. Microtubules are form birefringent.[17,38] The RNFL exhibits substantial linear birefringence with its slow axis parallel to the direction of nerve fiber bundles.[11-12,17,38] Near the optic nerve head, the slow axis distribution is nearly radial. The RNFL birefringence causes the speed of the polarized light to vary with the polarization orientation of the light. Inside the RNFL, the component with the polarization orientation parallel to the nerve fiber bundles propagates slower than the component with polarization perpendicular to the nerve fiber bundles; a relative phase shift is introduced. This phase shift is called retardation and is proportional to the RNFL birefringence and thickness (Fig. 2).

Retinal scanning laser polarimetry (SLP) was developed to assess the RNFL thickness, point by point in the peripapillary region, by measuring total retardation in the light reflected from the retina.[10-12,34] It was shown that RNFL retardation measured by SLP correlates well with thickness.[33] Near the ONH in a normal eye, retardation is higher in the superior and inferior regions and thinner in the temporal and nasal regions (Fig. 3 A), a pattern expected from the known anatomy of the eye. SLP is attractive because it provides an image, as well as rapid, objective, and reproducible assessment of the RNFL.

In the eye, the RNFL is not the only birefringent structure. The Henle fiber layer (HFL) in the macula is also birefringent. This layer consists of elongated photoreceptor axons, extending radially from the fovea. The HFL is structurally similar to the RNFL and exhibits linear birefrin-

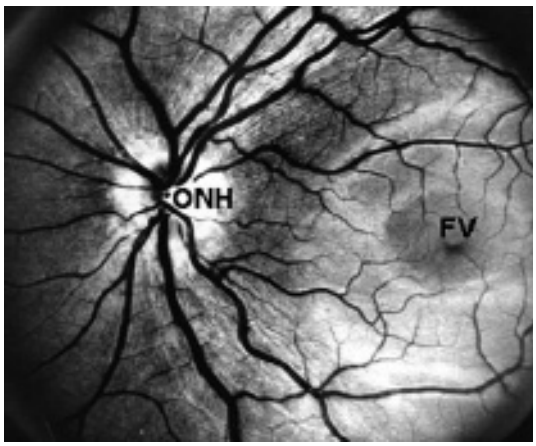

Fig.1. Red-free fundus photograph of a normal eye (OS). The bright striations converging towards the optic nerve head are nerve fiber bundles. ONH - optic nerve head. FV - fovea.

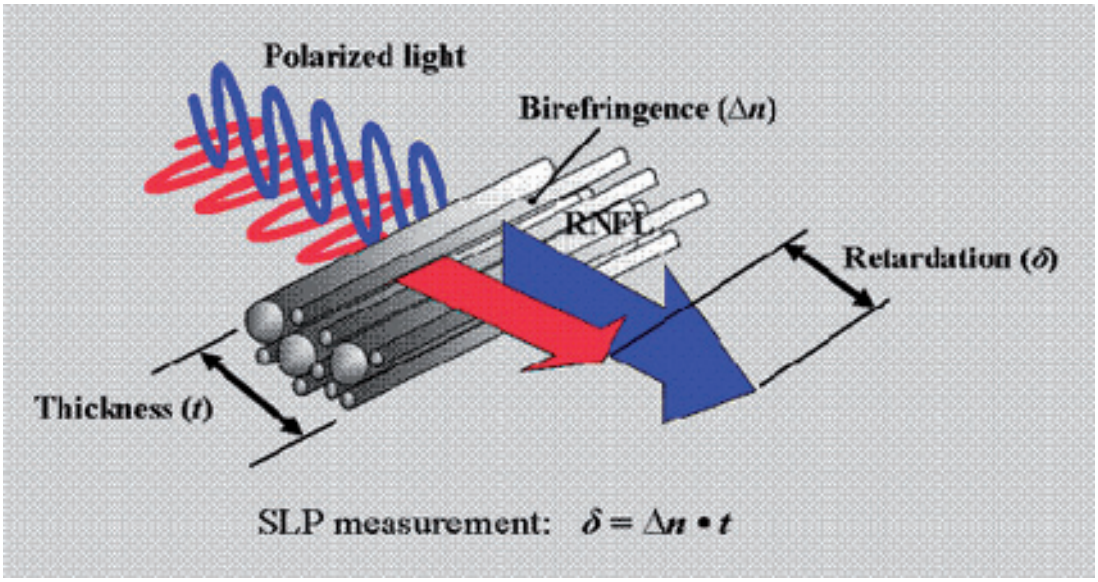

Fig. 2. Diagram illustrates the principle of RNFL assessment with SLP.

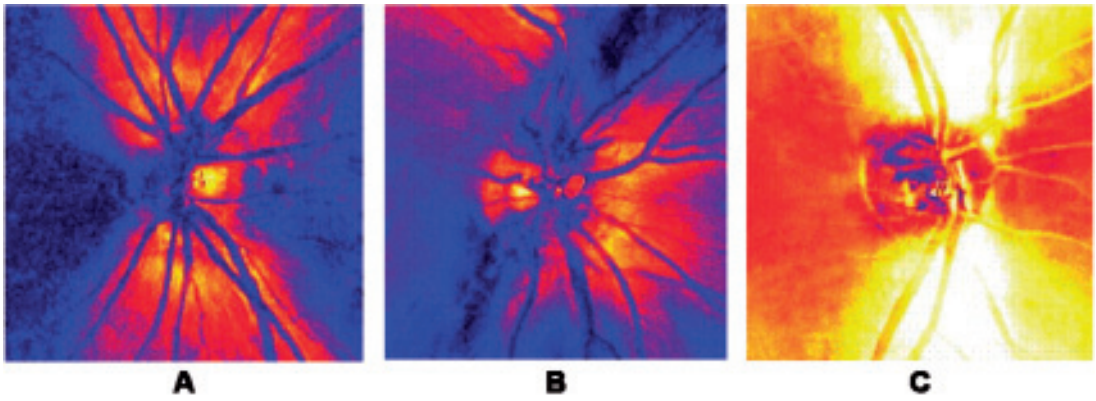

Fig. 3. The RNFL images of 3 normal eyes acquired with an earlier SLP system and fixed anterior segment compensation. The magnitude and axis of the anterior segment birefringence were very different for the 3 eyes, resulting in large variation in the RNFL measurement. A - RNFL image with good anterior segment compensation by FCC. B and C - RNFL images with poor anterior segment birefringence compensation by FCC.

gence with slow axes extending radially from the fovea.[3,6] The HFL is fairly uniform about the fovea. In addition to retinal birefringence, the anterior segment of the eye is also birefringent, mainly from the cornea and, to a lesser degree, from the lens.[4,32] Because all birefringent structures cause a change in the total retardation of a measurement beam, the accuracy of the RNFL measurement with SLP depends on the ability to extract the RNFL retardance from the measured total retardation. To minimize corneal and lens birefringence, a fixed corneal compensator (FCC) with 60 nm retardance and 15° nasally downward fast axis was employed in earlier commercial SLP systems. FCC compensated for anterior segment birefringence in some eyes effectively (Fig. 3 A) and failed in others (Fig. 3 B and 3 C). Consequently, the incomplete compensation contributes to the variability of RNFL assessment by SLP.[13-15,22] Studies of linear birefringence of the central human cornea have shown wide variation in both the retardance magnitude and birefringence axis among individuals.[21,35] Individualized anterior segment compensation

which accounts for the variation in both magnitude and axis is required for SLP measurements. Based on this need, a new commercial SLP system, GDx VCC (Laser Diagnostic Technologies, Inc.) was developed in which a variable corneal compensator (VCC) was employed to achieve individualized anterior segment compensation.[39-40] The radial birefringence of the Henle's fiber layer in the macula is used conveniently as an "intraocular polarimeter" for measurement of corneal birefringence, and VCC is adjusted for each eye to measure the RNFL. The effect of corneal compensation and clinical applications of GDx VCC are demonstrated in this paper.

METHODS

SLP MEASUREMENT

GDx VCC is a modified SLP system with variable corneal compensation. Images of the ocular fundus are formed by scanning the beam of a near-infrared laser (780 nm) in a raster pattern.[12,40] The scan raster covers an image field 40° horizontally and 20° vertically in the eye, covering both the peripapillary region and the macular region. SLP measurement models for human eye are described in details elsewhere.[12,20,22,39-40] Briefly, in GDx VCC, the eye is treated as a partial depolarizer in series with the anterior segment retarder and the retinal retarder.[40] As in earlier SLP systems, a GDx VCC measurement is made with linear polarized light. Light returned from the eye is usually elliptically polarized and is separated into two channels with linear analyzers parallel and perpendicular to the illuminating polarization. The plane of polarization and the two analyzers rotate to produce a series of images. For a single image pixel, the theoretical outputs of the two channels are illustrated in figure 4. The minimum of the crossed channel and the maximum of the parallel channel occur when the input polarization is aligned with either the slow axis or the fast axis of the retarder being measured.[12,20,40] Retardation of a single pixel is derived from the two outputs based on equation (1):[12,20,40]

$$\delta = \sin^{-1}\sqrt{\frac{2F_1}{P_{ave} + F_1 - d}} \qquad (1)$$

where
δ: Single-pass retardation in the beam path,
$2F_1$: Intensity modulation in the crossed channel,
F_0 : Average intensity of the crossed channel,
d : Depolarized light in the crossed channel,
P_{ave} : Average intensity of the parallel channel,
K : The totally polarized retinal reflectance ($K = P_{ave} + F_1 - d$).
Because noise is inevitable in actual measurement, F_1 and F_0 are obtained by Fourier analysis of the crossed channel output, with F_0 the DC term of the Fourier series, F_1 the amplitude of the fundamental, and depolarization component $d = F_0 - F_1$.
Birefringence axis is determined from the crossed channel signal. When polarization plane is aligned with either the fast axis or the slow axis of the net birefringence, light remains linearly polarized and the crossed channel signal intensity is minimum. From a single SLP measurement, one cannot differentiate the fast axis from the slow axis. The value in the axis image (θ) corresponds to the polarization plane 45° away from either the slow or the fast axis, where the crossed channel intensity is maximum. The axis value is always within the range of 0°~90°.
For each measurement, GDx VCC generates 4 images (Fig. 5): a fundus reflectance image (P_{ave}), a single-pass retardation image (δ), a birefringence axis image (θ), and a depolarized light image (d). Figure 5 illustrates the GDx VCC measurement of a normal subject. The 40° × 20° scan field of GDx VCC covers both the peripapillary region around the optic nerve head (ONH) and the macular region around the fovea (FV). Near the ONH, higher retardance is observed in the superior and inferior regions (Fig. 5 δ), corresponding to thicker RNFL, and birefringence axis distri-

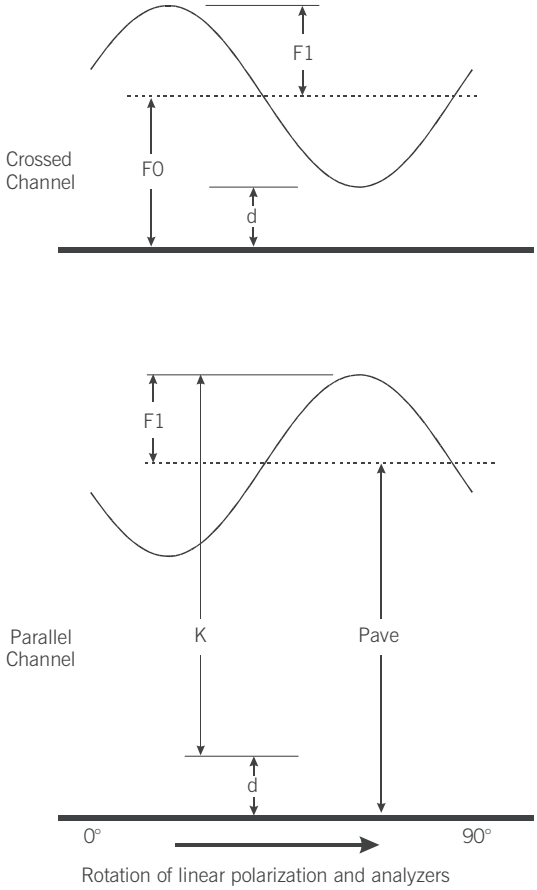

Fig. 4. Theoretical output of SLP model.

bution is nearly radial (Fig. 5 θ). Around the fovea, the Henle's fiber layer exhibits fairly uniform birefringence (Fig. 5 δ), and birefringence axes are radially distributed (Fig. 5 θ).

Corneal birefringence measurement

SLP measures total retardation in the beam path. Any residual birefringence from the anterior segment directly interferes with RNFL measurement. Because corneal birefringence is known to vary significantly from eye to eye,[21,35] fixed corneal compensation will only work in some eyes.[39] To achieve individualized corneal compensation, a variable corneal compensator (VCC) was implemented in GDx VCC.[40] The variable corneal compensator consists of two identical linear retarders in rotating mounts; both the retardance and axis of the VCC unit can be adjusted according to actual corneal birefringence.

In SLP, corneal birefringence refers to the total birefringence of the cornea and the lens. Since lens birefringence is usually weak, corneal birefringence is the main component. In general, corneal birefringence is modeled with a biaxial crystal, with one optic axis perpendicular to the corneal surface and another axis parallel to the corneal surface.[32] At normal incidence, the optic axis perpendicular to the corneal surface has no effect on the polarization state of the illuminating beam and therefore is negligible. Corneal birefringence is not uniform; usually retardance increases toward the periphery of the cornea.[7,32] In SLP, because the scan beams are approximately perpendicular to the corneal surface and cover only a small central area, the cornea is

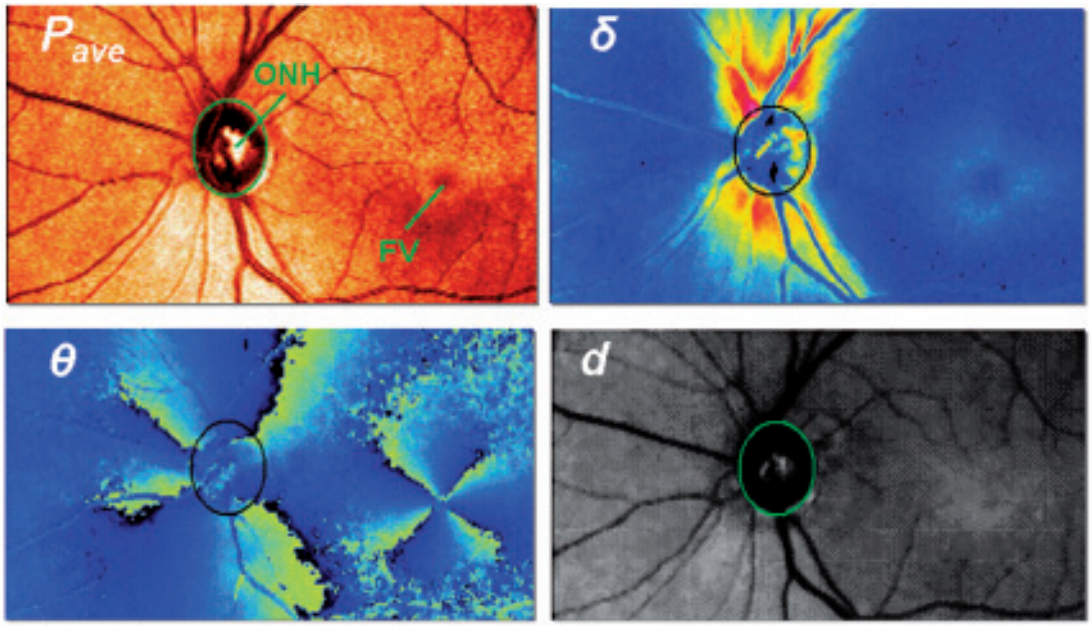

Fig. 5. Images generated from a GDx VCC measurement. Pave - Fundus reflectance image. δ - Single-pass retardance image. θ - Birefringence axis image. d - Depolarized light image. ONH - Optic nerve head. FV - Fovea.

well described as a uniform linear retarder with the optic axis parallel to the corneal surface.[4,21,32]

To determine corneal birefringence, an SLP image of the retina is acquired with VCC retardance set to zero. SLP measures the combination of two linear retarders, the cornea and the retina. In the macular region, the retinal retarder is the Henle's fiber layer with radial axes; in the peripapillary region, the retinal retarder is the RNFL with approximately radial axes. The radial birefringence of Henle's fiber layer in the macula is used as an intraocular polarimeter; SLP image of this structure without compensation allows determination of both the retardance and birefringence axis of the cornea.[39]

A linear retarder can be described by its retardance (δ) and the azimuth (θ) of its optic axis. Based on Mueller calculus, for a two-retarder combination, cornea (δ_C, θ_C) and retina (δ_R, θ_R), the combined retardance (δ) is determined as follows:

$$\cos(2\pi\delta/\lambda) = \cos(2\pi\delta_R/\lambda)\cos(2\pi\delta_C/\lambda) - \sin(2\pi\delta_R/\lambda)\sin(2\pi\delta_C/\lambda)\cos 2(\theta_R - \theta_C) \quad (2)$$

Based on this equation, the combined retardance varies with the angle between the azimuths of the two retarders. When θ_R - θ_C is 0°, the two axes of the retarders are completely aligned with each other; the total retardance is then the sum of the two retarders ($\delta = \delta_R + \delta_C$), maximum retardance of the combination. When θR - θC is 90°, the two axes of the retarders are perpendicular to each other; the total retardance is then the difference of the two retarders ($\delta = \delta_R - \delta_C$), minimum retardation of the combination.

Based on equation (2), in an SLP image for corneal measurement (VCC retardance set to 0 nm), the combination of the radial Henle's fiber layer and the uniform cornea should form a bow-tie pattern in the macula. Corneal birefringence measurement of a normal eye is illustrated in figure 6. A bow-tie pattern is observed in the macula in the SLP retardation image. The orientation of the bow-tie pattern is aligned with the slow axis of the cornea. A macular retardation profile is obtained at a locus of points along a circle centered on the fovea (indicated by the dotted red circle in figure 6). Assuming radial axes of the Henle's fiber layer, corneal birefringence axis, corneal retardance, and the Henle's fiber layer retardance can all be determined through least-

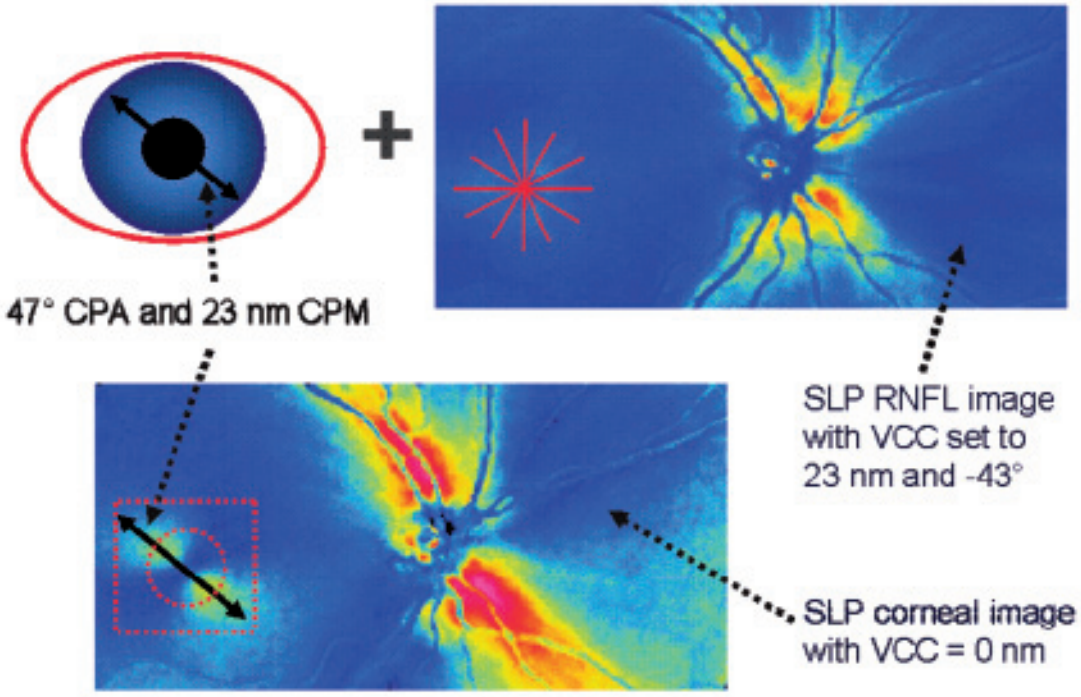

Fig. 6. Corneal birefringence measurement of an healthy eye from macula retardation profile (red dotted circle in SLP corneal image with VCC set to 0 nm). The Henle's fiber layer is treated as a linear retarder with radial axes and the cornea is treated as a linear retarder with single axis. CPA - Corneal polarization axis. CPM - Corneal polarization magnitude.

squares fit of equation (2) to the macular retardation profile.[39] When corneal birefringence is well compensated, SLP measures only the retinal retardance, and macular retardance pattern is fairly uniform (Fig. 6, top right image), as expected from the anatomy of the eye.

In addition to the corneal measurement method based on the macular "bow-tie" pattern as described above, a "screen" method for calculating corneal birefringence is also implemented in GDx VCC.[20,40] While the "bow-tie" method is robust for eyes with a normal macula, corneal polarization axis measurement may not be accurate in eyes with severely damaged Henle's fiber layer.[2] The "screen" method is simply another set of calculations performed on the same SLP image for corneal measurement (with VCC set to 0 nm). The working hypothesis is that in the absence of macular birefringence, the fundus of the eye acts as a polarization-preserving screen that displays the anterior segment birefringence.[20] By averaging the signals from the parallel channel and crossed channel over a large area of the macula, the impact of irregularities of the retinal birefringence is greatly reduced and corneal birefringence can be extracted.[20] In GDx VCC, the screen method is performed over a square area centered on the fixation point (dotted red square in figure 6).

From each SLP corneal measurement image, corneal birefringence values are calculated and saved in the patient database based on the "bow-tie" method and the "screen" method, respectively. The operator decides which set to use based on the patient's macular condition. For most eyes corneal birefringence values derived through the two methods are nearly identical.

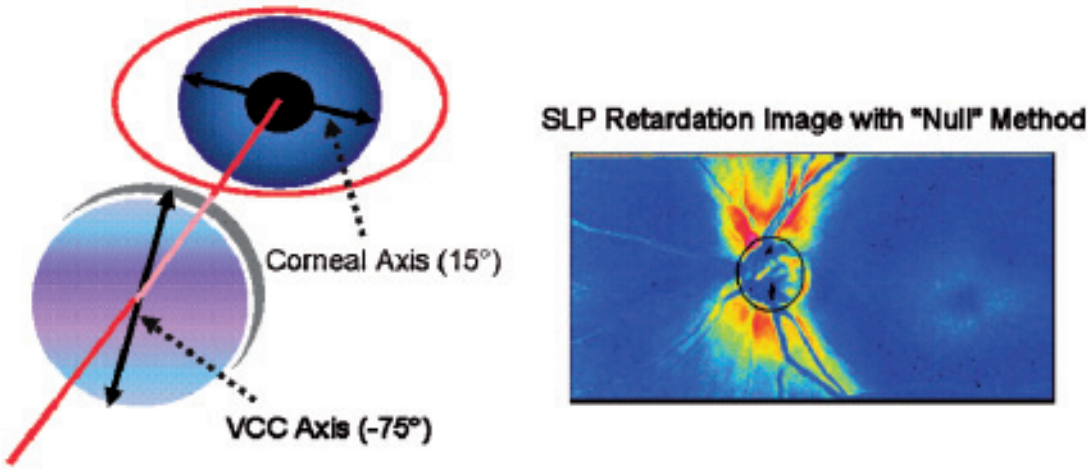

Fig. 7. Illustration of SLP RNFL imaging with the ''Null'' corneal compensation method.

Corneal birefringence compensation with the ''null'' method and the ''bias'' method

Once corneal birefringence is known, direct corneal compensation can be achieved by birefringence cancellation with the variable corneal compensator (VCC); the magnitude of the VCC is set to the same value of cornea retardance and the slow axis of the VCC is set to be perpendicular to the slow axis of the cornea, as illustrated in figure 7. This birefringence cancellation method, named in this paper as the ''Null'' method, is currently implemented in GDx VCC systems as the default compensation method. With the ''Null'' method, the total retardation in SLP RNFL image is directly the RNFL retardance. Typically, RNFL retardance is in the range of 0 nm ~ 90 nm.

As an alternative to the ''Null'' method, a new software method was developed that requires no hardware modification to the GDx VCC system and provides individualized corneal compensation with enhanced SLP measurement sensitivity. Based on equation (1), the sensitivity of SLP in measuring small retardation differences ultimately depends on the detection of small differences in polarization signal amplitude F_1. SLP sensitivity (the slope of the curve) is inherently low at low retardance as shown in figure 8. Depolarization or reduction in reflected light intensity results in a lower curve and proportionally decreased sensitivity, as illustrated with the curves for $K = 1.0$ and $K = 0.5$. Low sensitivity makes the retardation measurement susceptible to error, both optical (e.g., stray light) and electronic (e.g., noise, digitization error). The principle of the new method, illustrated in Fig. 8, is to superimpose the RNFL birefringence onto a large, known birefringence (''bias retarder''). The bias retarder is formed by the combination of the VCC and the cornea. Rather than adjusting VCC to cancel corneal birefringence, the VCC is adjusted so that the combination has retardance close to 55 nm and slow axis close to vertical. The bias retarder shifts the retardation measurement into a more sensitive region (Fig. 8). The new method is named ''Bias'' method in this paper and also known as ''ECC'' method in the GDx VCC system software.

With the ''Bias'' method, SLP measures higher total retardation (δ_{total}) than RNFL retardance alone and the birefringence axis image (θ_{total}) is continuous across the entire image (Fig. 9) due to the large bias. The continuous axis image is important in the ''Bias'' method because the ambiguity of differentiating the slow axis from the fast axis in a single SLP measurement is eliminated. The bias retarder can be decomposed into a rotator with rotation angle of $\delta\theta$ and a linear retarder with retardance of δ_{bias} and optic axis of θ_{bias}.[19] The linear retarder portion of the bias

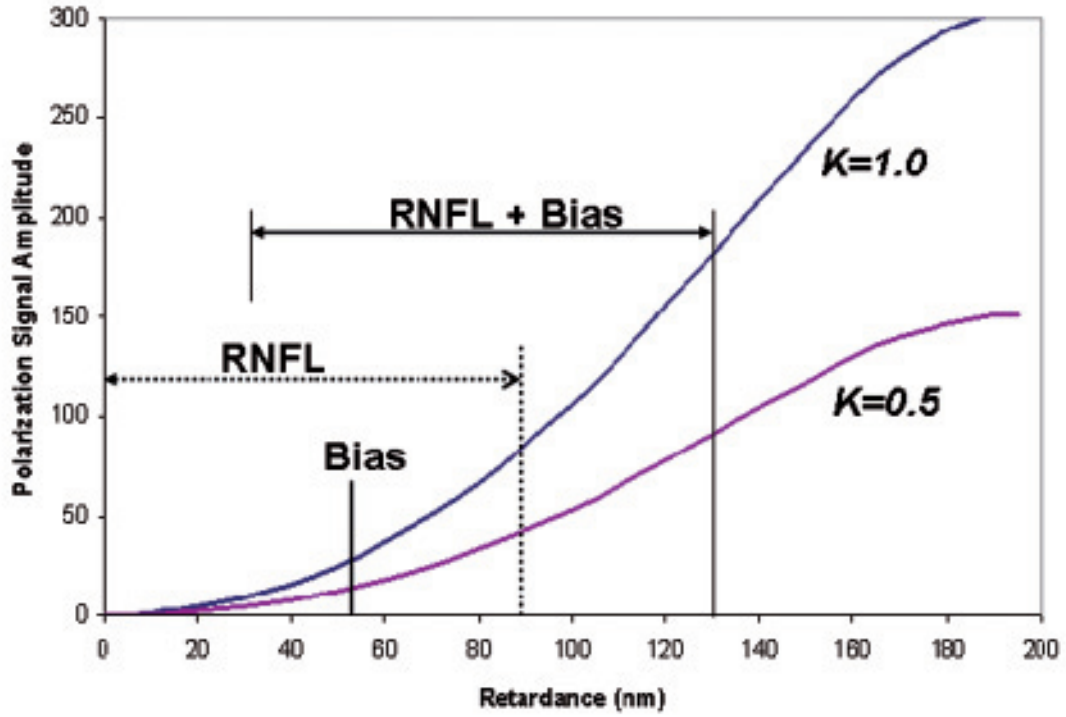

Fig. 8. SLP measurement sensitivity characteristics.

retarder (δ_{bias} and θ_{bias}) is determined from the macular region using the "screen" method described earlier. Based on Mueller calculus for double-pass SLP system, the retinal retardance (δ_{RNFL}) is mathematically determined as:

$$\cos\left(2\delta_{RNFL}\right) = A^2C + 2ABDE - B^2\left(F^2 + CE^2\right) \qquad (3)$$

where

A: $A = \cos\delta_{Bias}$,
B: $B = \sin\delta_{Bias}$,
C: $C = \cos 2\delta_{Total}$,
D: $D = \sin 2\delta_{Total}$,
E: $E = \cos 2(\theta_{Total} - \theta_{Bias})$,
F: $F = \sin 2(\theta_{Total} - \theta_{Bias})$,

Notice that the retinal retardance calculation is independent of the rotation ($\Delta\theta$). Retinal retardance is calculated, point by point, across the entire image to produce the final RNFL image (Fig. 9) based on equation (3). Bias retardance is successfully removed from the final retinal retardation image, evident from the uniform retardation pattern in the macula.

RNFL analysis and normative database

GDx VCC provides objective assessment of the RNFL through spatially resolved retardation measurement and comparison of the RNFL measurement with an established RNFL normative database. GDx VCC clinical data were collected from multiple eye clinics, following an IRB approved study protocol with clearly defined inclusion and exclusion criteria for enrollment. The subjects were enrolled into two groups: 1) normal subjects, and 2) subjects with glaucoma. The protocol

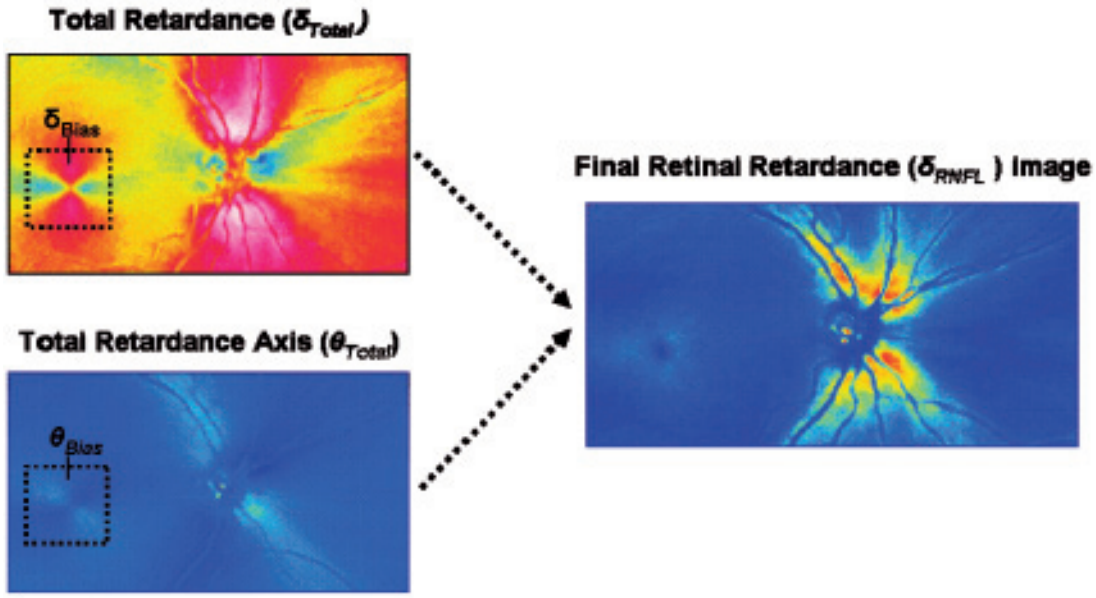

Fig. 9. Illustration of corneal compensation with "Bias" method.

included criteria for medical and ophthalmic history, family history of glaucoma, intraocular pressure, visual field test results, optic disc appearance, etc. All subjects recruited were at least 18 years of age. The multi-center clinical data served several purposes: validate GDx VCC technology, build a normative database, and develop a machine learning classifier to assist glaucoma diagnosis.

A machine learning classifier was created using a machine learning technique called Support Vector Machine (SVM); SVM is a form of supervised artificial intelligence. The SVM-based classifier created for GDx VCC is named Nerve Fiber Indicator (NFI). NFI was trained with two clinically predefined groups, RNFL measurements of normal eyes and RNFL measurements of glaucomatous eyes, to create a decision boundary between the two groups. The range of the NFI output is from 0 to 100; a value lower than 30 indicates a normal eye and a value higher than 30 usually indicates a glaucomatous eye.

The main RNFL measurements are: peripapillary RNFL retardation profile plotted in the order of temporal, superior, nasal, inferior, and temporal (TSNIT curve), TSNIT average, Superior Average, and Inferior Average. The measurements are compared to the normative database establish based on the multi-center data and parameters fall outside the normal range is highlighted in colours based on probability values. Examples of RNFL analysis report of a normal subject and a glaucoma subject are provided in figure 10.

RESULTS

Variable corneal compensation reduces retinal retardation measurement variation

Based on the anatomy of the eye, in a normal eye, the RNFL is thicker in the superior and inferior peripapillary region and thinner in the inferior and temporal regions. Further, the Henle's fiber layer is fairly uniform around the fovea. Because retinal retardance is proportional to the thickness of the retinal birefringent structures, the SLP retardation image is expected to be uniform around the fovea and exhibits higher retardance in the superior and inferior peripapillary

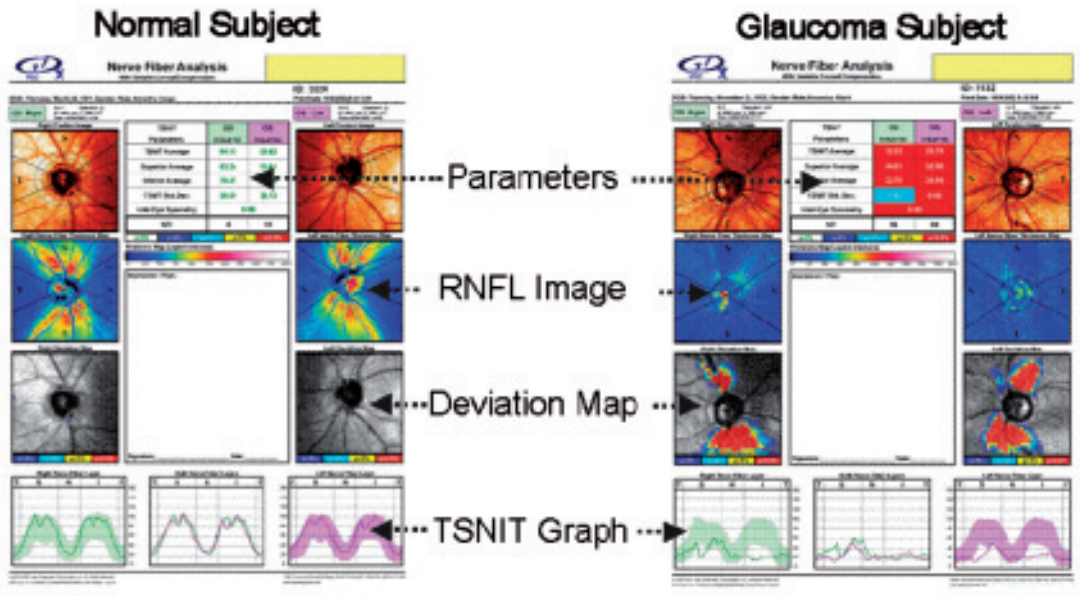

Fig. 10. Examples of GDx VCC RNFL analysis report which includes RNFL retardance image, deviation of RNFL distribution from normative range at each super pixel (Deviation Map), parameter table with comparison to the normative database, machine learning classifier (NFI), and TSNIT graphs with normative range.

regions. Figure 11 illustrates the impact of variable corneal compensation in SLP measurement via side-by-side comparison of four normal eyes imaged with fixed corneal compensation (FCC) and variable corneal compensation (VCC) respectively. The corneal retardance of the four eyes ranged from 33 nm to 88 nm and the corneal birefringence axis ranged from 9° to 55° nasally downward. In FCC images, there were large variations in retardation patterns, both in the peripapillary region and the macula. As discussed earlier, a bow-tie pattern in the macula indicates a bias birefringence from the anterior segment, FCC failed in all but one eye. In VCC images, however, the RNFL patterns were similar from eye to eye and the macula retardation patterns were fairly uniform around the fovea for all four eyes. RNFL measurement variability was reduced and individualized corneal compensation was achieved with VCC.

''Null'' method and ''bias'' method comparison

The "Null" method and the "Bias" method both achieved individualized corneal compensation as shown in figure 12. The RNFL retardation images by the two methods were nearly identical (top and middle rows in figure 12); however, the retardation images with the "Bias" method appeared to have improved signal-to-noise ratio. The "Bias" method also appeared to reduce SLP measurement artifacts observed in some retardation images with the "Null" method (bottom row in figure 12).

GDx VCC identifies glaucomatous RNFL defects

Glaucoma induced RNFL damage can be categorized into two types, focal defect (i.e. wedge defect) and diffuse defect. Both types are readily identified in the visual RNFL image provided by GDx VCC as demonstrated in figure 13 with images of a normal eye (Fig. 13 A) and three eyes with glaucoma (Fig. 13 B, 13 C, and 13 D). The insets are corresponding visual field pattern deviation maps (Fig. 13 A, 13 B, and 13 C) and visual field total deviation map (Fig. 13 C). Healthy RNFL, as shown in figure 13 A, is thicker in superior and inferior, and thinner in tem-

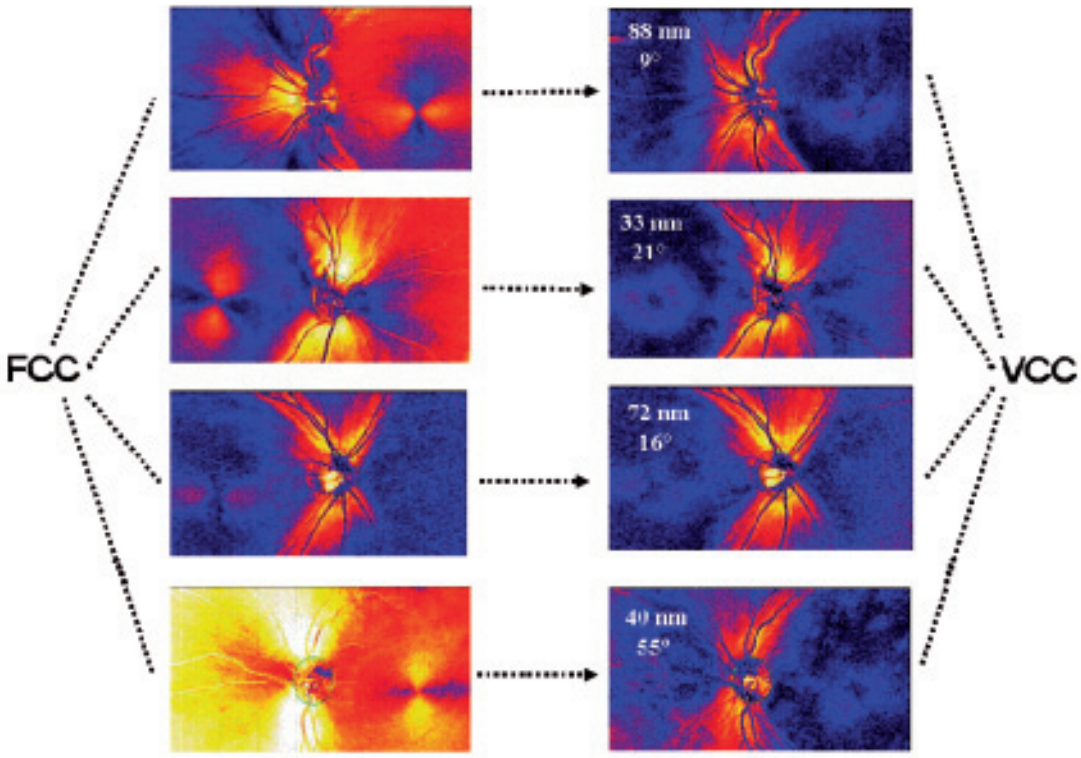

Fig. 11. Side-by-side comparison of four normal eyes imaged with fixed corneal compensation (FCC) and variable corneal compensation (VCC) respectively. The corneal retardance of the eyes ranged from 33 nm to 88 nm and the corneal birefringence axis ranges from 9° to 55° nasally downward. VCC clearly reduced the RNFL measurment variability and achieved individualized corneal compensation, evident from the much similar RNFL retardance patterns among the 4 eyes and the uniform macular retardance pattern.

poral and nasal, and good symmetry is usually observed between superior and inferior quadrants. The visual field pattern deviation map is normal for this eye. Figure 13 B shows GDx VCC retardation image of a glaucoma eye with superior-temporal focal RNFL damage; inferior visual field loss was found in the pattern deviation map, corresponding to the RNFL damage. Figure 13 C shows another glaucoma eye with extensive inferior RNFL damage; severe superior visual field loss was found in the pattern deviation map, again corresponding to the RNFL damage. Finally, figure 13 D shows a glaucomatous eye with advanced diffuse RNFL damage; advanced global visual field loss was found in the total deviation map. Glaucomatous RNFL damage measured with GDx VCC appears to correlate with visual field damage.

Detection of early stage glaucoma with the aid of normative database and neural network

Since RNFL damage is the earliest sign of glaucoma, GDx VCC is potentially capable of detecting glaucoma prior to visual field damage measured with standard automated perimetry. Figure 14 demonstrates one clinically confirmed early glaucoma case in which RNFL damage was clearly identified in both eyes with GDx VCC and through comparison with normative database and NFI (Fig. 14 A). However, both the total deviation map and the pattern deviation map of visual field test were still normal (Fig. 14 B).

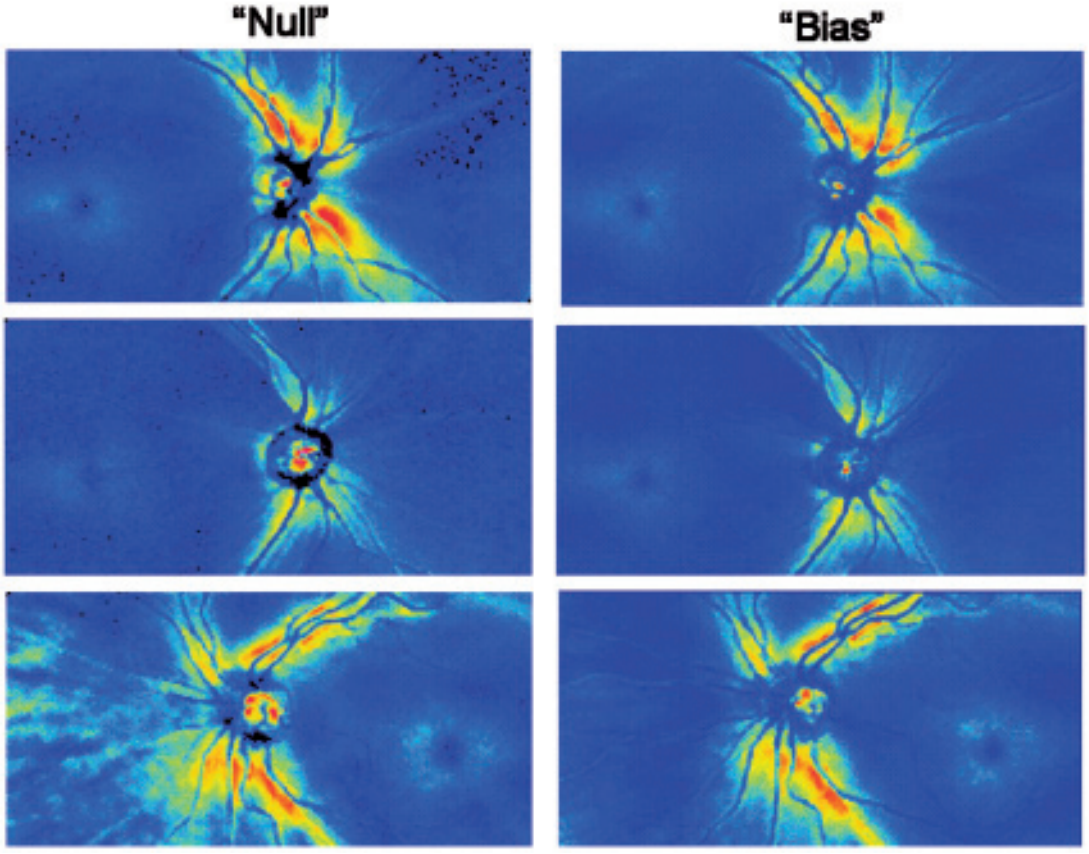

Fig. 12. Side-by-side comparison of GDx VCC retardation images by ''Null'' method and ''Bias'' method respectively. The top row is a normal subject, the middle row is a glaucoma subject, and the bottom row is another normal subject.

DISCUSSIONS

Individualized corneal compensation is achieved with GDx VCC. Glaucomatous RNFL damage can be detected effectively with the new SLP technology. Normative database and machine learning classifier allow diagnosis from a single exam. Quantitative and reproducible RNFL assessment with GDx VCC, as well as the significant association between the RNFL measurement and visual field deviation in glaucomatous eyes, suggest that GDx VCC may also be a tool to monitor progression of the disease.

GDx VCC measures retardation resulting from polarized light double-passing the RNFL. In principle, retardation is proportional to both the RNFL birefringence and the RNFL thickness. However, to convert retardation to actual thickness requires an accurate value for RNFL birefringence. The recently reported variation in birefringence around the ONH has consequences for the interpretation of GDx VCC results.[8,18] GDx VCC measurements are reported as RNFL thickness values using a fixed conversion factor in the instrument. This conversion is performed to simplify the communication with clinicians. However, it also causes some confusion in understanding the GDx measurement. If birefringence is not constant, then the thickness values derived from retardation based on fixed conversion may not be interpreted as actual RNFL anatomical thickness. However, the clinical utility of GDx VCC does not depend on providing direct thickness measurement. The clinical utility of SLP retardation measurement in detecting glauco-

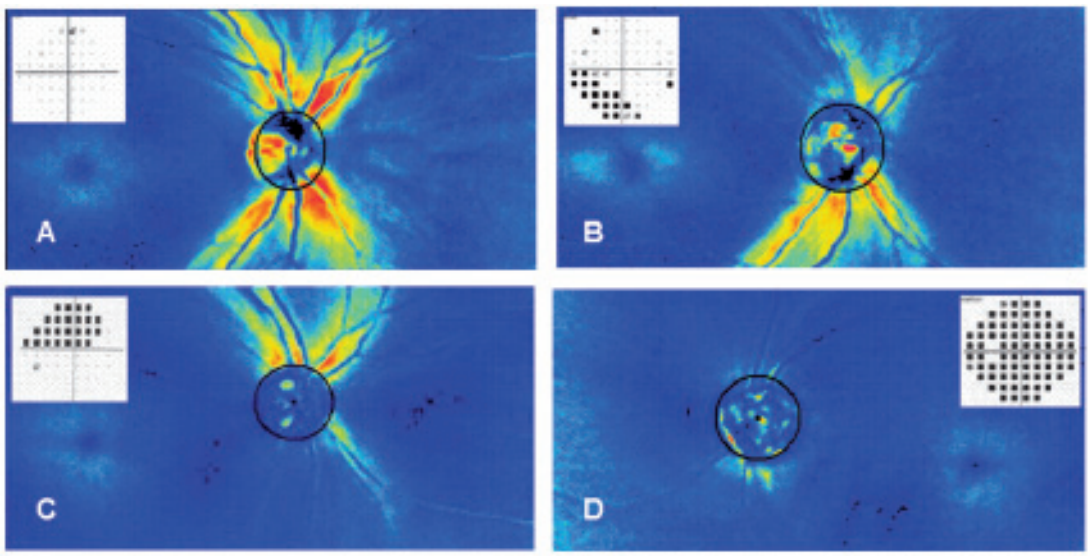

Fig. 13. GDx VCC RNFL retardation images of a normal eye (A) and eyes with glaucoma (B, C, and D). The insets are visual field pattern deviation maps (in A, B, and C) and visual field total deviation map (in C) for the 4 eyes respectively. A - Normal eye with normal RNFL and normal visual field. B - glaucoma eye with superior-temporal focal RNFL damage, corresponding to inferior visual field loss. C - glaucoma eye with extensive inferior RNFL damage, corresponding to severe superior visual field loss. D - glaucoma eye with advanced diffuse RNFL damage, corresponding to advanced global visual field loss.

matous RNFL damage has been validated in various clinical studies.[1,5,9,23,27-29,31,36-37] The ability to detect wedge defects is significantly improved with GDx VCC, and the wedge defects in GDx VCC RNFL images agree well with observations based on red-free fundus photographs.[27] Using GDx VCC to successfully detect RNFL damage in eyes with experimental glaucoma was reported by Weinreb et al.[36] The ability to discriminate between normal and glaucomatous RNFL is improved significantly with GDx VCC. High sensitivity and specificity are reported in a number of clinical studies.[9,23,29,31,37] GDx VCC RNFL measurements are also found to correlate with visual field sensitivities [5,28] and RNFL thickness measurement by optical coherence tomography.[1] These studies have demonstrated that retardation is a clinically relevant quantity for assessing glaucomatous RNFL damage.

As suggested in recent articles,[8,18] the RNFL ultrastructure may be affected in glaucoma and result in RNFL birefringence change. Since retardation is a product of thickness and birefringence, GDx VCC provides a readily available clinical tool to detect change in both thickness and birefringence, without differentiating one from the other. Further, the clinical utility of GDx VCC does not depend on its reported measurement units; comparison of SLP parameters with normative database and comparison of a follow-up exam with baseline measurement in an individual are valid.

ACKNOWLEDGEMENTS

The author thanks Robert N. Weinreb (MD), Robert W. Knighton (PhD), and Xiang-Run Huang (PhD), for valuable discussions on the corneal compensation methods. The author also acknowledges Pak-Wai Lo, William Papworth, Peter Trost (PhD), Ryan Betts, Guoqiang Li (PhD), Jerry Reed, George Gayda, Dan McCreary, Rick Bienias, Ross Winnick, Haedeuk Yae, Jim Wilburn, Charlie Wallace, Shawnnah Castillo, Daniel Bolish, Kitty Legerton, William Simons, Mike Sinai (PhD), William Wong, Moe Blais, and John Moore for their contributions to the development of the GDx VCC product.

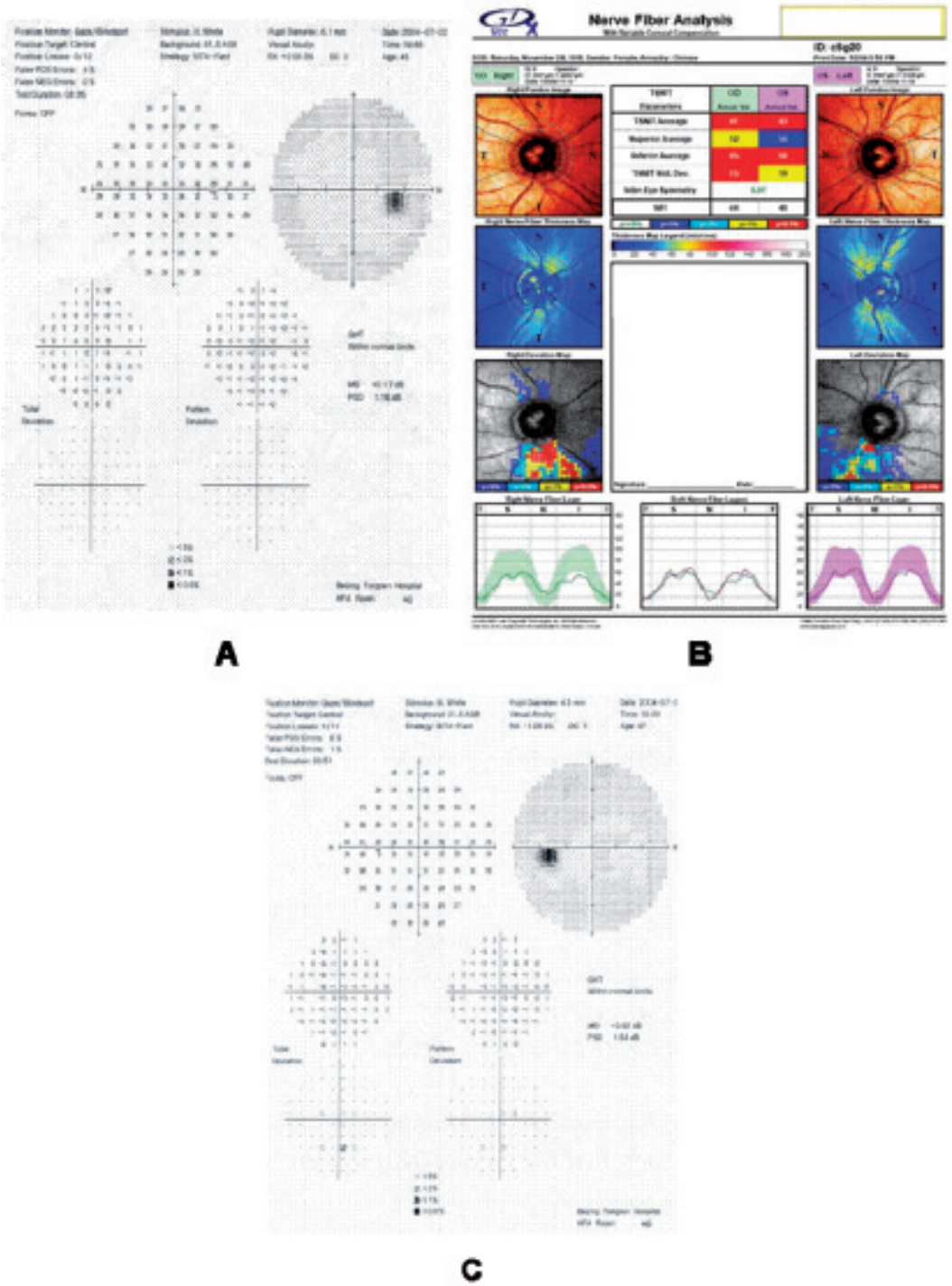

Fig. 14. Case example of an early stage glaucoma patient. B - Diffuse RNFL damage was identified in GDx VCC report: flagged parameters, high NFI values, flagged deviation maps, and TSNIT plots outside normative range. A & C - Visual field report was normal for both the right eye and the left eye.

REFERENCES

(1) BAGGA H., GREENFIELD D.S., FEUER W., KNIGHTON R.W. – Scanning laser polarimetry with variable corneal compensation and optical coherence tomography in normal and glaucomatous eyes. Am J Ophthalmol 2003; 135: 521-529

(2) BAGGA H., GREENFIELD D.S., KNIGHTON R.W. – Scanning laser polarimetry with variable corneal compensation: identification and correction for corneal birefringence in eyes with macular disease. Invest Ophthalmol Vis Sci 2003; 44: 1969-1976

(3) BONE R.A., LANDRUM J.T. – Macula pigment in Henle fiber membranes: a model for Haidinger's brushes. Vis Res 1984; 24: 103-108

(4) BOUR L.J. – Polarized light and the eye. In: Charman W.N. (ed.) Visual Optics and Instrumentation. CRC Press, Boca Raton, FL 1991; 310-325

(5) BOWD C., ZANGWILL L.M., WEINREB R.N. – Association between scanning laser polarimetry measurements using variable corneal polarization compensation and visual field sensitivity in glaucomatous eyes. Arch Ophthalmol 2003; 121: 961-966

(6) BRINK H.B., VAN BLOKLAND G.J. – Birefringence of the human foveal area assessed in vivo with Muller-matrix ellipsometry. J Opt Soc Am 1988; 5: 49-57

(7) BUENO J.M. – Measurement of parameters of polarization in the living human eye using imaging polarimetry. Vision Res 2000; 40: 3791-3799

(8) CENSE B., CHEN T.C., PARK B.H., PIERCE M.C., DE BOER J.F. – Thickness and birefringence of healthy retinal nerve fiber tissue measured with polarization-sensitive optical coherence tomography. Invest Ophthalmol Vis Sci 2004; 45: 2606-2612

(9) CHOPLIN N.T., ZHOU Q., KNIGHTON R.W. – Effect of individualized compensation for anterior segment birefringence on retinal nerve fiber layer assessments as determined by scanning laser polarimetry. Ophthalmol 2003; 110: 719-725

(10) DREHER A.W., REITER K. – Retinal laser ellipsometry: a new method for measuring the retinal nerve fiber layer thickness distribution? Clin Vision Sci 1992; 7: 481-488

(11) DREHER A.W., REITER K. – Scanning laser polarimetry of the retinal nerve fiber layer. Proc SPIE 1992; 1746: 34-41

(12) DREHER A.W., REITER K., WEINREB R.N. – Spatially resolved birefringence of the retinal nerve fiber layer assessed with a retinal laser ellipsometer. Appl Opt 1992; 31: 3730-3735

(13) GARWAY-HEATH D.F., GREANEY M.J., ROZIER M., CAPRIOLI J. – Estimation and correction of the corneal component of retardation with the scanning laser polarimeter for glaucoma diagnosis. Invest Ophthalmol Vis Sci 2000; 41: S121 (ARVO Abstract 620)

(14) GREENFIELD D.S., KNIGHTON R.W., HUANG X.R. – Effect of corneal polarization axis on assessment of retinal nerve fiber layer thickness by scanning laser polarimetry. Am J Ophthalmol 2000; 129: 715-722

(15) GREENFIELD D.S., KNIGHTON R.W., FEUER W.J., SCHIFFMANN J.C., ZANGWILL L., WEINREB R.N. – Correction for corneal polarization axis improves the discriminating power of scanning laser polarimetry. Am J Ophthalmol 2002; 134: 27-33

(16) HOYT W.H., FRISEN L., NEWMAN N.M. – Fundoscopy of nerve fiber layer defects in glaucoma. Invest Ophthalmol 1973; 12: 814-829

(17) HUANG X.R., KNIGHTON R.W. – Linear birefringence of the retinal nerve fiber measured in vitro with a multispectral imaging micropolarimeter. J Biomed Opt 2002; 7: 199-204

(18) HUANG X.R., BAGGA H., GREENFIELD D.S., KNIGHTON R.W. – Variation of peripapillary retinal nerve fiber layer birefringence in normal human subjects. Invest Ophthalmol Vis Sci 2004; 45: 3073-3080

(19) HURWITZ H., JONES R.C. – A new calculus for the treatment of optical systems. II. Proof of the three general equivalence theorems. J Opt Soc Am 1941; 3: 493-499

(20) KNIGHTON R.W., HUANG X.R. – Analytical methods for scanning laser polarimetry. Optics Express 2002; 20: 1179-1189

(21) KNIGHTON R.W., HUANG X.R. – Linear birefringence of the central human cornea. Invest Ophthalmol Vis Sci 2002; 43: 82-86

(22) KNIGHTON R.W., HUANG X.R., GREENFIELD D.S. – Analytical model of scanning laser polarimetry for retinal nerve fiber layer assessment. Invest Ophthalmol Vis Sci 2002; 43: 383-392

(23) MEDEIROS F.A., ZANGWILL L.M., BOWD C., BERND A.S., WEINREB R.N. – Fourier analysis of scanning laser polarimetry measurements with variable corneal compensation in glaucoma. Invest Ophthalmol Vis Sci 2003; 44: 2606-2612
(24) QUIGLEY H.A., MILLER N.R., GEORGE T. – Clinical evaluation of nerve fiber layer atrophy as an indicator of glaucomatous optic nerve damage. Arch Ophthalmol 1980; 98: 1564-1571
(25) QUIGLEY H.A., ADDICKS E.M., GREEN W.R. – Optic nerve damage in human glaucoma. Arch Ophthalmol 1982; 100: 135
(26) QUIGLEY H.A., KATZ J., DERICK R.J., GILBERT D., SOMMER A. – An evaluation of optic disc and nerve fiber layer examinations in monitoring progression of early glaucoma damage. Ophthalmol 1992; 99: 19-28
(27) REUS N.J., COLEN T.P., LEMIJ H.G. – Visualization of localized retinal nerve fiber layer defects with the GDx with individualized and with fixed compensation of the anterior segment birefringence. Ophthalmol 2003; 110: 1512-1516
(28) REUS N.J., LEMIJ H.G. – The relationship between standard automated perimetry and GDx VCC measurements. Invest Ophthalmol Vis Sci 2004; 45: 840-845
(29) SHIRAKASHI M., YAOEDA K., FUKUSHIMA A., FUNAKI S., FUNAKI H., OFUCHI N., NAKATSUE T., ABE H. – Usefulness of GDx VCC in glaucoma detection. Journal of the Eye 2003; 20: 1019-1021
(30) SOMMER A., KATZ J., QUIGLEY H.A., MILLER N.R., ROBIN A.L., RICHTER R.C., WITT K.A. – Clinically detectable nerve fiber atrophy precedes the onset of glaucomatous field loss. Arch Ophthalmol; 109: 77-83
(31) TANNENBAUM D.P., HOFFMAN D., LEMIJ H.G., GARWAY-HEATH D.F., GREENFIELD D.S., CAPRIOLI J. – Variable compensation improves discrimination between normal and glaucomatous eyes with the scanning laser polarimeter. Ophthalmol 2004; 111: 259-264
(32) VAN BLOKLAND G.J., VERHELST S.C. – Corneal polarization in the living human eye explained with a biaxial model. J Opt Soc Am 1987; 4: 82-90
(33) WEINREB R.N., DREHER A.W., COLEMAN A., QUIGLEY H., SHAW B., REITER K. – Histopathologic validation of Fourier-ellipsometry measurements of retinal nerve fiber layer thickness. Arch Ophthalmol 1990; 108: 557-560
(34) WEINREB R.N., SHAKIBA S., ZANGWILL L. – Scanning laser polarimetry to measure the nerve fiber layer of normal and glaucomatous eyes. Am J Ophthalmol 1995; 119: 627-637
(35) WEINREB R.N., BOWD C., GREENFIELD D.S., ZANGWILL L.M. – Measurement of the magnitude and axis of corneal polarization with scanning laser polarimetry. Arch Ophthalmol 2002; 120: 901-906
(36) WEINREB R.N., BOWD C., ZANGWILL L.M. – Scanning laser polarimetry in monkey eyes using variable corneal compensation. Journal of Glaucoma 2002; 11: 378-384
(37) WEINREB R.N., BOWD C., ZANGWILL L.M. – Glaucoma detection using scanning laser polarimetry with variable corneal polarization compensation. Arch Ophthalmol 2003; 121: 218-224
(38) ZHOU Q., KNIGHTON R.W. – Light scattering and form birefringence of parallel cylindrical arrays that represent cellular organelles of the retinal nerve fiber layer. Appl Opt 1997; 36: 2273-2285
(39) ZHOU Q., WEINREB R.N. – Individualized compensation of anterior segment birefringence during scanning laser polarimetry. Invest Ophthalmol Vis Sci 2002; 43: 2221-2228
(40) ZHOU Q., REED J., BETTS R., TROST P. – Detection of glaucomatous retinal nerve fiber layer damage by scanning laser polarimetry with variable corneal compensation. SPIE Ophthalmic Technologies XIII 2003; 4951: 1-10

.....

Corresponding address:

Qienyuan Zhou, PhD
R&D
Carl Zeiss Meditec Inc
10805 Rancho Bernardo Rd, Ste 210
San Diego, CA 92127-5703
UNITED STATES
Phone: (858)716-0678
Email: q.zhou@meditec.zeiss.com